이학석사 학위논문

Prognostic implications and interaction of LINE-1 methylation and p53 expression statuses in advanced gastric cancer

진행성 위암에서의 LINE-1 메틸화와 p53 발현의 상호작용과 예후에 미치는 영향

2019년 2월

서울대학교 대학원
의과대학 종양생물학 전공

신 윤 주

Prognostic implications and interaction of LINE-1 methylation and p53 expression statuses in advanced gastric cancer

지도교수 강 경 훈

이 논문을 이학석사 학위논문으로 제출함
2018년 10월

서울대학교 대학원
의과대학 종양생물학 전공
신 윤 주

신윤주의 이학석사 학위논문을 인준함
2019년 1월

Chair _____(Seal)
Vice Chair _____(Seal)
Examiner _____(Seal)

Abstract

Prognostic implications and interaction of LINE-1 methylation and p53 expression statuses in advanced gastric cancer

Yun-Joo Shin
Department of Cancer Biology
Seoul National University College of Medicine

Known as a tumor suppressor protein, p53 regulates multiple essential biological processes that prevent tumorigenesis, including DNA repair, cell cycle arrest, senescence, angiogenesis, and induction of apoptosis. The *TP53* gene is frequently mutated across various tissue types of cancers. In addition to losing its wild type function, gain of function p53 mutation gives a selective advantage for tumor maintenance and progression. Long interspersed nuclear element-1 (LINE-1, L1) are repetitive DNA elements comprising approximately 17% of the human genome. L1 expression is mostly repressed by methylation of CpG sites in 5' untranslated region in somatic cells but is activated by DNA demethylation process during tumorigenesis. Since L1 has retrotransposition activity, active L1 can

contribute to genomic instability, which is one of the hallmarks of malignancy. On the other hand, p53 is indispensable for maintaining genomic stability. Other studies have identified that p53 plays its role in controlling genomic stability by repressing retrotransposon activity. However, the regulatory functions of p53 related to L1 are largely unknown in human gastric cancer (GC). It is also unclear whether p53 regulates L1 expression differently depending on the mutational status of p53. Through investigating p53 expression by immunohistochemistry and L1 methylation level by pyrosequencing, we identified a strong correlation between L1 methylation and p53 expression. To this end, we hypothesized that p53 expression can influence L1 expression or L1 methylation and that p53 can affect L1 methylation differently depending on mutational status of *TP53*. In this study, we examined the mechanism by which p53 controls the expression and methylation levels of L1 in *TP53*-deleted KATOIII and *TP53* wild type AGS human gastric cancer cell line. Notably, two types of mutant p53 (V143A and R249S) repressed L1 retrotransposition activity but R175H mutant did not. Also, L1 methylation level tended to be different depending on the type of *TP53* mutation. A further study is required to elucidate the underlying mechanism of our findings.

Keyword: p53, LINE-1, methylation, pyrosequencing, epigenetics, gastric cancer, KATOIII

Student Number: 2017-29457

Table of Contents

List of Tables

List of Figures

Introduction

Gastric cancer (GC) is the fifth most common malignant tumor and the third leading cause of cancer-related death worldwide. Despite advances in technology, the diagnosis and treatment of gastric cancer still remains as a challenge(1). The current TNM staging serves well for the selection of treatment and assessment of prognosis. However, survival time varies in patients with advanced gastric cancer within the same stage, which indicates that the current TNM staging system is not sufficient for the prognosis estimation. Development of prognostic biomarkers might ameliorate the prognostication power of the current staging system.

Long interspersed nuclear element-1 (LINE-1, L1) is a retrotransposon which is repeated a half million times in an interspersed manner and comprises about 17% of the human genome. Promoter CpG island hypermethylation is an important mechanism for the suppression of gene expression and retrotransposon activity. Cancer cells tend to undergo diffuse hypomethylation which leads to the increased activity of L1 retrotransposon(2, 3). Hypomethylation of L1 may contribute to genomic instability and tumorigenesis(4). DNA hypomethylation in the promoter and 5' untranslated region of L1 repeats has been demonstrated to be closely associated with worse recurrence-free survival and overall survival in patients with gastric cancer(5).

Somatic mutation of *TP53* gene is one of the most frequent

alternation in human cancer, and its germline mutation is the cause of Li-Fraumeni syndrome, which invokes early onset cancer(6). Overall, 50% of human cancers contains *TP53* mutation, and negative regulators of p53, MDM2 and MDM4, are frequently increased in remnant cases(7). In most cases of *TP53* mutation, a single amino acid is substituted in the DNA binding domain, which leads to loss of function despite the protein length being intact(8, 9). Loss of function in *TP53* gene is known to lose the function of regulating cell cycle checkpoint and inducing apoptosis by its protein p53(10). In spite of the fact that *TP53* is largely accepted as a tumor suppressor gene, oncogenic effect of mutant p53 proteins, including deregulated metabolic pathway, increased tumor invasion, and enhanced chemotherapy resistance, has also been reported, indicating a gain of function role for mutant p53(10-13). One of the mechanisms involving gain of function in *TP53* mutation includes upregulation of epigenetic genes, especially genes that serve as histone methyltransferases and acetyltransferases, via binding to the transcription factor. A recent study by Zhu et al. has demonstrated that *MLL1, MLL2,* and *MOZ* were upregulated in human tumor samples with *TP53* gain of function mutations, but not when *TP53* was wild type or null status (9). However, the effect of p53 in other epigenetic regulators, including promoter methylation status of L1, is still elusive.

To date, it is well established that L1 is hypomethylated in many cancers and causes genomic instability. Also, p53 acts as a guardian

against transposopathy, which maintains genomic stability of the cell by restraining transposable element such as L1(14). However, the correlation between L1 methylation and p53 expression is largely unknown in human gastric cancer. Also, it is unclear whether difference in mutational status of p53 affects L1 expression or not. In the present study, we investigated the correlation between p53 expression and L1 methylation level to determine whether expression status or mutational status of *TP53* influences expression and methylation status of L1 in gastric cancer tissue and cell lines.

Materials and Methods

Patient specimens

492 formalin-fixed paraffin embedded (FFPE) samples of advanced gastric cancer (AGC), defined by gastric cancer with the invasive depth of at least the muscularis propria (pT2-pT4 according to the 7th cancer staging system of the American Joint Committee on Cancer), were collected from the pathological archive of Seoul National University Hospital. All samples were selected from patients who received resection of AGC between January 2007 and December 2008. Clinical data were obtained from the electronic medical record retrospectively. The age of patients ranged from 23 to 86 (mean age of 61). Male to female ratio was 2.09:1. This study was approved by the Institutional Review Board of Seoul National University Hospital, which waived the requirements to obtain informed patient consent. Among the samples, 451 were adequate for measurement of L1 methylation level.

Detection of molecular subtypes

All AGC samples were tested for microsatellite instability (MSI) and Epstein-Barr Virus (EBV) infection. For MSI status, 5-marker scoring panel (*BAT25, BAT26, D2S123, D5S345, and D17250*) was applied. MSI-high (MSI-H) was defined when instability was detected in greater than or equal to 40% of markers. Other cases were

categorized as MSI-negative. EBV-positive AGC was detected via in situ hybridization with RNAscope FFPE assay kit (Advanced cell Diagnostics, Inc.) that target *EBER1*.

Extraction of genomic DNA from archival tissue samples

FFPE blocks containing each patient sample were cut with 10-μm thickness and attached to glass slides. Slides were soaked into xylene followed by air dry. Tumor areas of each slide was traced from tumor areas marked from its H&E counterpart and microdissected with a razor blade into 50μL of lysis buffer including 10% proteinase K. Dissected tissues were incubated in 56°C for at least 24 hours. Proteinase K was inactivated by heat block at 95°C for 30 minutes.

Tissue microarray (TMA) and immunohistochemistry

Through microscopic examination of a pathologist (YK), representative areas that contain considerable amount of tumor were selected and core tissues (2-mm in diameter) were extracted for each AGC FFPE sample. These cores were rearranged to a new recipient block using a trephine apparatus to form TMA blocks. For immunohistochemical staining, FFPE sections of TMA were socked in xylene for deparaffinization and were rehydrated with gradual decrease of alcohol concentration. Sections were immunostained after antigen retrieval. Primary antibody for anti-p53 (DAKO, clone DO-7) was stained at a concentration of 1:1000. Intensity of p53

expression within tumor cells was measured for each core. The proportion of tumor cells with moderate/strong nuclear staining for *TP53* was estimated by light microscopic examination of two tissue cores (3- mm in diameter) for each patient sample. Tumors were defined as p53 group 3 and 2 when >90% and 90-50% of tumor cells showed moderate/strong nuclear staining, respectively. p53 group 1 denoted samples with moderate/strong nuclear staining in less than 50% of tumor cells or samples with weak nuclear staining. p53 negativity (p53 group 0) was defined as no staining of tumor cells which was contrasted with weak nuclear staining of interstitial lymphocytes. All virtual slides were viewed and judged independently by two pathologists (YK and GHK) according to three-tiered scale without knowledge of clinical outcome.

Cell culture and growth media

The human gastric cancer cell lines including AGS and KATOIII were purchased from Korean Cell Line Bank (Seoul, Korea) and were cultured in a humidified, 5% CO_2 incubator at 37℃. Cells were grown in RPMI-1640 supplemented with 10% heat-inactivated Fetal bovine serum, 100U/ml penicillin, and 100μg/ml streptomycin. Culture medium was replaced approximately every 48hrs.

Plasmid DNA used in transfection assay

Plasmids encoding wild type human p53 and mutant type p53 (V143A, R175H, and R249S) under the control of the CMV promoter (pCMV-

NEO-BAM vector) were provided as a gift from Cancer Genomics Research Laboratory (Cancer Research Institute, Seoul, Korea). The pLRE3-mEGFP1(monomeric enhanced green fluorescent protein) plasmid, encoding a retrotransposition- competent L1, and pJM111-LRE3-mEGFP1, encoding a retrotransposition-defective L1, were gifts from Dr, Moran (University of Michigan Medical school). This retrotransposition- competent L1 plasmid contains an active human L1 with an mEGFP1 (Monomeric Enhanced Green Fluorescent Protein) retrotransposition indicator cassette in its 3' untranslated region. The pJM111-LRE3-mEGFP1, retrotransposition-defective L1 plasmid, is identical to pLRE3-mEGFP1 except for two missense mutations in ORF1p (RR261-262AA). pCMV6-Entry (that includes G418-resistance gene) plasmid was used as a control DNA.

p53 knockdown using shRNA (short hairpin RNA) lentiviral plasmid

Plasmids expressing control shRNA (#H1(shRNA-Ctr)-RB) and shRNA against human *TP53* (#LVP343-RB) were purchased from GenTarget Inc. (San Diego, USA). The plasmid contains RFP (Red Fluorescence Protein)-Bsd (Blasticidin) dual selection marker. AGS cells were transduced with pre-made lentiviral plasmid containing control shRNA and p53 shRNA. Three days after transduction, cells were incubated with RPMI-1640 complete medium containing 6 μg/ml blasticidin (RPMI-Bsd). For generating cells stably expressing control shRNA and p53 shRNA, single cells expressing RFP were

sorted by BD FACS (Fluorescence-activated cell sorter) Aria II into individual wells of 96 well plates. Several single colonies were screened by light microscope, selected, and transferred to individual wells in 48-well dishes and expanded in RPMI-Bsd media. Stable knockdown of p53 expression was confirmed by western blot.

Generation of stable cell line

AGS and KATOIII cells were transfected with the pLRE3-mEGFP1 and pJM111-LRE3-mEGFP1 construct by electroporation (NEPA GENE) and selected for puromycin resistant cells. Antibiotic selection was initiated 48hr after transfection. Puromycin-resistant cells were selected by growth in RPMI-1640 complete medium containing 0.3 μg/ml and 0.4 μg/ml puromycin (RPMI-Puro) for AGS and KATOIII. After complete antibiotic selection, the cells were trypsinized and plated at low density in 6-well plates. EGFP-expressing clones were observed by fluorescence microscopy. Several fluorescent colonies were selected, transferred to individual wells in 6-well dishes and expanded in RPMI-Puro. KATOIII cells stably expressing L1 were then transfected with the pCMV-Neo-Bam-wild type p53, pCMV-Neo-Bam-p53 V143A, pCMV-Neo-Bam-p53 R175H, and pCMV-Neo-Bam-p53 R249S by electroporation (NEPA GENE). Stable clones expressing wild type, three types of mutant type p53, and control vector were selected with G418 (400μg/ml). After complete antibiotic selection, the cells were trypsinized and plated at low density in 6-well dishes. Several visible

colonies were picked, transferred to individual wells in 6-well dishes and expanded in RPMI-G418 media. The colonies were screened for their presence by western blot, reverse transcription (RT)-polymerase chain reaction (PCR), and PCR using the pCMV vector-specific oligonucleotides [5'-ATA ATA CCG CGC CAC ATA GC-3' (forward, Amp-R) and 5'-CCG GGA GCT GCA TGT GTC AGA GG-3' (reverse, pGEX 3')] and p53-specific oligonucleotides [5'-TTC TGG GAC AGC CAA GTC TG-3' (forward) and 5'- CAC GCA CCT CAA AGC TGT TC-3' (reverse)]. Meanwhile, AGS cells stably expressing L1 were transduced with lentiviral plasmid expressing p53 shRNA and single cells were sorted by BD FACS Aria II. Wild type and three types of mutant type p53 were then transfected into AGS stably expressing L1 and p53 shRNA. G418 selection and confirmation of transfection were done as described above.

RNA preparation and RT-PCR

Total RNA was extracted from cell lines using QIAGEN RNeasy Mini Spin Columns, according to the manufacturer's protocol (QIAGEN). 1μg of total RNA was reverse-transcribed into cDNA using the LeGene Express 1st Strand cDNA Synthesis System kit (LeGene). Reverse transcription-polymerase chain reaction (RT-PCR) was performed in a 25μl final volume containing 2 μl of qualified cDNA, 1x CoralLoad PCR Buffer, 0.2mM of dNTP, 0.4 μM of the forward primer, 0.4 μM of the reverse primers, and 0.75U of HotStarTaq Plus DNA polymerase (Qiagen). The PCR cycling conditions were as

follows: initial denaturation at 95℃ for 10 minutes, 35 cycles of 94℃ for 40 seconds, 57℃ for 40 seconds, and 72℃ for 40 seconds followed by a final extension at 72℃ for 5 minutes. The primers for amplification of human *TP53* gene were as follows: 5'-TTC TGG GAC AGC CAA GTC TG-3' (forward) and 5'- CAC GCA CCT CAA AGC TGT TC-3' (reverse). Glyceraldehyde-3-phosphate dehydrogenase (GAPDH) primers were used as internal positive controls. PCR products were then observed at 2.5% agarose gels for confirmation.

Western blot analysis

Cells were lysed with RIPA buffer supplemented with protease inhibitor cocktail (Complete Mini, Roche) and phosphatase inhibitor cocktail (PhosSTOP EASYpack, Roche). Cell debris were then removed by centrifugation at 4℃. After centrifugation, protein concentrations were measured by BCA protein assay (Pierce). For western blotting, 30μg of protein lysates from each established cell lines were separated by 8~10% SDS-polyacrylamide gel electrophoresis (PAGE), transferred onto nitrocellulose membranes (Millipore), blocked at room temperature for 1hr with 5% skim milk and incubated at 4℃ overnight with the following primary antibodies: p53 (1:1000, sc-126, Santa Cruz Biotechnology), β-actin (1:1000, sc-47778, Santa Cruz Biotechnology) and EGFP (1:1000, ab184601, Abcam). After three 15 minute washes with Tris-buffered saline containing 0.1% Tween 20, the blots were incubated at room

temperature for 1hr with horseradish peroxidase-conjugated secondary antibody: goat anti-Mouse IgG(H+L)-HRP (1:4000, #SA001-500, GenDEPOT). Proteins were detected using chemiluminescent reagent, ECL solution (#W6002, Biosesang)

DNA preparation and bisulfite conversion.

Genomic DNA was extracted from cell lines using the QIAamp DNA mini kit (Qiagen). DNA samples were then digested in 20μl reaction volumes with 15U of HindIII (TaKaRa) for 1hr at 37℃ prior to bisulfite modification. Bisulfite modification was performed using the Zymo EZ DNA methylation Kit (Zymo Research) with 500ng of digested genomic DNA according to the manufacturer's protocol.

MethyLight assay

After bisulfite modification, Alu-based MethyLight control reaction, a CpG-independent and bisulfite specific control reaction, was performed to measure input bisulfite-modified DNA(15). We determined threshold cycle [C(t) value] of this reaction in which the Alu reaction fluorescence was detected. To keep the C(t) value of bisulfite-modified DNA samples in the range of 18 to 20, distilled water was added to dilute bisulfite-modified DNA samples with C(t) values lower than 18. MethyLight PCR reaction was carried out in a 25μl final volume comprised of 0.2mM dNTPs, 0.3μM forward and reverse PCR primers, 0.1μM probe, 3.5mM $MgCl_2$, 0.01% Tween-20, 0.05% gelatin, and 0.2 units of Taq polymerase on a 384-well plate

(BioRad). The PCR cycling conditions were as follows: initial denaturation at 95℃ for 10 minutes, then 50 cycles of 95℃ for 20 seconds followed by 59℃ for 40 seconds.

Pyrosequencing methylation assay

The sodium bisulfite-modified DNA samples were amplified with the same oligonucleotide primers which were designed against a consensus L1 sequence by the Issa group for pyrosequencing(16). The oligonucleotides used for PCR were 5'-TTTTGAGTTAGGTGTGGGATATA (forward primer) and 5'-biotin-AAAATCAAAAAATTCCCTTTC (reverse primer). The polymerase chain reactions were performed in a 25μl final volume containing 2 μl of bisulfite-treated DNA, 1x CoralLoad PCR Buffer, 3mM of $MgCl_2$, 0.2mM of dNTP, 0.4 μM of the forward and biotinylated reverse primers and 0.75U of HotStarTaq Plus DNA polymerase (Qiagen). The PCR cycling conditions were as follows: initial denaturation at 95℃ for 10 minutes, 50 cycles of 94℃ for 30 seconds, 57℃ for 30 seconds, and 72℃ for 30 seconds followed by a final extension at 72℃ for 5 minutes. PCR products were then observed at 2.5% agarose gels for confirmation. In a pyrosequencing experiment, the binding buffer (Qiagen) and the Streptavidin Sepharose High Performance beads (GE healthcare Bio-Sciences Corp., Uppsala, Sweden) were added to the PCR products. The biotinylated DNA-bound beads were collected and denatured using denaturation buffer (Qiagen) in the PyroMark Vacuum Prep WorkStation (Qiagen). Next,

the purified single-stranded PCR product was added to the annealing buffer (Qiagen) which was mixed with 0.3 μM of sequencing primer (5'-AGTTAGGTGTGGGATATAGT), and the pyrosequencing reaction was performed using the PyroMark Q24 platform (Qiagen). The level of methylation at each of the four CpG sites [CpG sites 1-4: nucleotide positions 328, 321, 318, and 306 of X58075(GeneBank accession number)] was measured by the percentage of methylated cytosines relative to the sum of C and T nucleotides at each CpG site. The pyrosequencing assay was repeated in triplicate, and the mean value of the three replicates was reported as the representative value of L1 methylation.

FACS analysis

For FACS analysis, cells were prepared by washing with 3ml phosphate-buffered saline (PBS) followed by trypsinization of the adherent cells with 1ml of 0.05% trypsin-EDTA (Gibco). Cells were harvested by centrifugation at 1000rpm for 5min and were resuspended with FACS buffer (1x PBS with 0.5% BSA) and transferred to polystyrene tubes by passage through cell strainer caps (Falcon) and kept on ice until FACS analysis. Total $1x10^5$ cells were analyzed by a FACS CantoII flow cytometer (BD bioscience) equipped with a blue laser (488nm) and 525/50nm emission filter.

Statistical analysis

All statistical analysis was performed by R (version 3.5.1). The

correlation between categorical variables was performed with chi-square test when all categories were more than 5. If at least one category was equal to or less than 5, Fisher exact test was applied. Correlation between continuous variables and two categories were measured by student t-test. ANOVA was performed between variables that included more than two categories. Mann–Whitney U test (Wilcoxon rank-sum test) was applied when relationship between continuous variables and variables with more than two categories were measured. Univariate survival was determined by Kaplan-Meier curve with a log rank test. To calculate multivariate survival, Cox regression model was applied. P value of < 0.05 was considered as significant.

Results

L1 methylation level and p53 expression statuses in AGC

p53 expression was categorized into four groups according to overall intensity of cells as described in previous section; loss of expression (group 0, Figure 1A), weak to moderate expression (group 1, Figure 1B), moderate to strong expression (group 2, Figure 1C), and strong expression in all tumor cells (group 3, Figure 1D). High L1 methylation level was strongly correlated with p53 intensity group 1 in total AGC cohort ($P < 0.01$), but other three groups did not show significant difference in L1 methylation levels (Figure 2A). MSI-negative, EBV-negative AGCs also had similar results, as p53 group 1 intensity associated with high L1 methylation level (Figure 2B). In MSI-H and EBV-positive AGC populations, however, relatively small number of samples for each group undermined the correlation between p53 intensity and L1 methylation (Figure 2C to 2D).

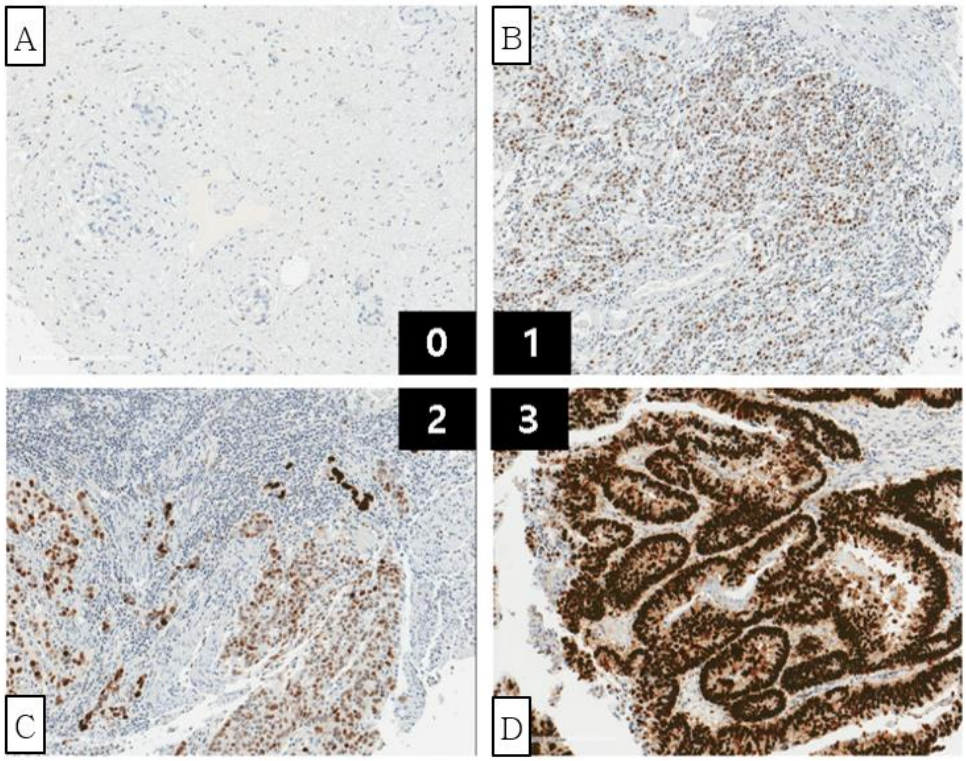

Fig. 1. Classification of p53 intensity by immunohistochemical staining

(A) p53 negativity (group 0)

(B) Moderate/strong nuclear staining in less than 50% of tumor cells or samples with weak nuclear staining (group 1)

(C) 90-50% of tumor cells showed moderate/strong nuclear staining (group 2)

(D) >90% of tumor cells showed moderate/strong nuclear staining (group 3)

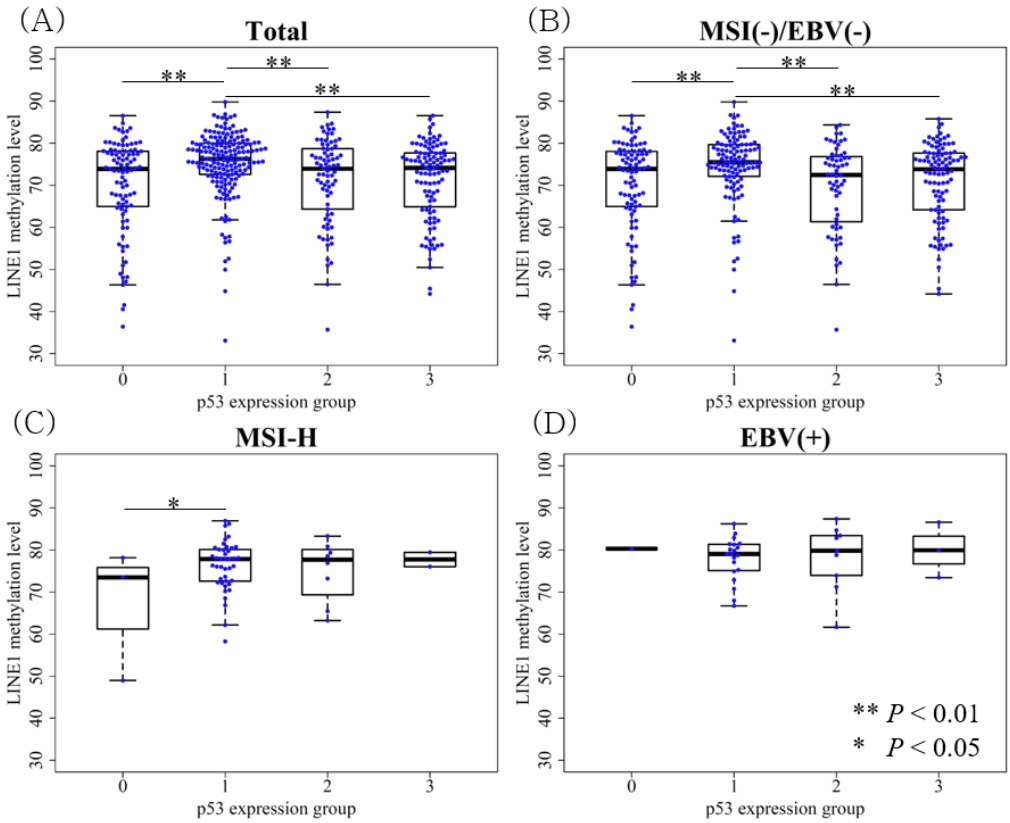

Fig. 2. Correlation between p53 expression and L1 methylation level measured by pyrosequencing

(A) All molecular subtype AGC included (B) MSI-negative, EBV-negative AGC samples (C) MSI-High AGC samples (D) EBV-positive AGC samples

Correlation between L1 methylation level, p53 intensity and clinicopathological characteristics

L1 methylation level was significantly associated various clinicopathological features as we have previously reported (Figure 3)(5, 17). Significantly correlated variables include age, sex, lymphatic invasion, venous invasion, Lauren's classification, pN stage, tumor differentiation, and molecular phenotypes, MSI-H and EBV-positive AGCs. Correlation between intensity of p53 and clinicopathological characteristics were measured with two different classification schemes (Table 1). When correlation across all four p53 intensity groups and clinicopathological features were determined via ANOVA, none of the observed values were statistically significant ($P > 0.05$). Since p53 intensity group 1 showed significant increase in L1 methylation level, we also compared features between group 1 and three other intensity groups (group 0, 2, and 3). Intensity group 1 was associated with poor tumor differentiation ($P < 0.05$) but had less lymph node metastasis compared with all other intensity groups ($P = 0.008$). Moreover, local invasions including lymphatic invasion and venous invasion was much less frequent in intensity group 1 ($P < 0.001$ and $P = 0.034$, respectively). Molecular subtypes with DNA hypermethylation, MSI-H and EBV-positive AGC, were frequently observed in p53 intensity group 1 than all other intensity groups combined ($P < 0.001$ and $P = 0.005$, respectively).

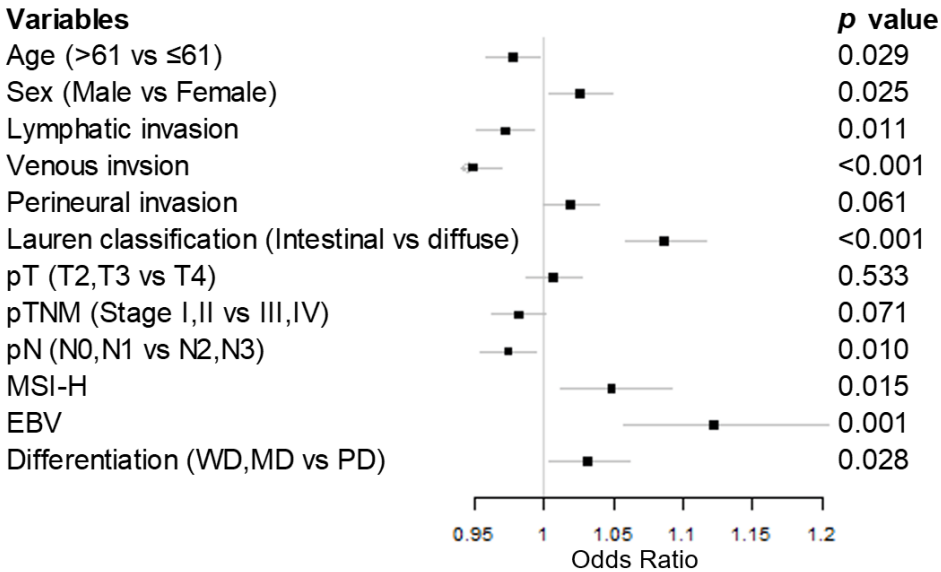

Fig. 3. Forest plot displaying relationships between L1 methylation level and clinicopathological characteristics.

Table 1. Intensity of p53 and clinicopathological variables

	p53 Intensity	0 (%)	1 (%)	2 (%)	3 (%)	*P* value (ANOVA)	*P* value (1 vs 0,2,3)
Sex						0.453	0.090
	Male	70 (14.3)	117 (23.9)	66 (13.5)	79 (16.1)		
	Female	33 (6.7)	69 (14.1)	18 (3.7)	38 (7.8)		
Age						0.927	0.809
	>61	46 (9.39)	91 (18.57)	40 (8.164)	58 (11.84)		
	≤61	57 (11.63)	95 (19.39)	44 (8.98)	59 (12.04)		
Tumor differentiation						0.174	0.025*
	Well	2 (0.4)	5 (1.0)	0 (0)	2 (0.4)		
	Moderate	27 (5.5)	38 (7.8)	27 (5.5)	32 (6.5)		
	Poor	18 (3.7)	72 (14.7)	30 (6.1)	31 (6.3)		
	Poorly cohesive	35 (7.1)	53 (10.8)	15 (3.1)	39 (8)		
	Others	21 (4.3)	18 (3.7)	12 (2.4)	13 (2.7)		
Lauren classification						0.538	0.052
	Intestinal	48 (9.8)	58 (5.9)	32 (6.5)	46 (9.4)		
	Diffuse	44 (9.0)	99 (11.8)	36 (7.3)	56 (11.4)		
	Mixed	11 (2.2)	29 (5.9)	16 (3.3)	15 (3.1)		
pT						0.390	0.390
	pT2	26 (5.3)	44 (9)	18 (3.7)	26 (5.3)		
	pT3	38 (7.8)	73 (14.9)	31 (6.3)	39 (8.0)		
	pT4a	33 (6.7)	63 (12.9)	29 (5.9)	49 (10.0)		
	pT4b	6 (1.2)	6 (1.2)	6 (1.2)	3 (0.6)		
pN						0.352	0.008*
	pN0	29 (5.9)	72 (14.7)	22 (4.5)	25 (5.1)		
	pN1	12 (2.4)	34 (6.9)	18 (3.7)	27 (5.5)		
	pN2	22 (4.5)	30 (6.1)	19 (3.9)	21 (4.3)		
	pN3a	26 (5.3)	27 (5.5)	18 (3.7)	27 (5.5)		
	pN3b	14 (2.9)	23 (4.7)	7 (1.4)	17 (3.5)		

(cont'd)

	p53 Intensity	0 (%)	1 (%)	2 (%)	3 (%)	*P* value (ANOVA)	*P* value (1 vs 0,2,3)
pTNM						0.407	0.090
	IB	16 (3.3)	30 (6.1)	7 (1.4)	10 (2.0)		
	IIA	13 (2.7)	39 (8.0)	12 (2.4)	16 (3.3)		
	IIB	11 (2.2)	26 (5.3)	21 (4.3)	24 (4.9)		
	IIIA	13 (2.7)	27 (5.5)	7 (1.4)	12 (2.4)		
	IIIB	18 (3.7)	21 (4.3)	14 (2.9)	21 (4.3)		
	IIIC	18 (3.7)	23 (4.7)	15 (3.1)	22 (4.5)		
	IV	14 (2.9)	20 (4.1)	8 (1.6)	12 (2.4)		
Lymphatic invasion						0.097	< 0.001**
	Absent	29 (5.9)	93 (19.0)	27 (5.5)	31 (6.3)		
	Present	74 (15.1)	93 (19.0)	57 (11.6)	86 (17.6)		
Venous invasion						0.214	0.034*
	Absent	66 (13.5)	149 (30.4)	61 (12.5)	89 (18.2)		
	Present	37 (7.6)	37 (7.6)	23 (4.7)	28 (5.7)		
Perineural invasion						0.056	0.348
	Absent	56 (11.4)	78 (15.9)	42 (8.6)	44 (9.0)		
	Present	47 (9.6)	108 (2.0)	42 (8.6)	73 (14.9)		
MSI						0.085	< 0.001**
	Stable	86 (17.6)	128 (2.4)	71 (14.5)	98 (20.0)		
	Low	14 (2.9)	13 (2.7)	5 (1.0)	16 (3.3)		
	High	3 (0.6)	45 (9.2)	8 (1.6)	3 (0.6)		
EBV						0.898	0.005*
	Absent	102 (20.8)	164 (33.5)	74 (15.1)	114 (23.3)		
	Present	1 (0.2)	22 (4.5)	10 (2.0)	3 (0.6)		

MSI: microsatellite instability; EBV: Epstein-Barr Virus

$*P < 0.05$; $**P < 0.01$

Survival analysis

In previous studies(5, 17), we have established tumoral L1 hypomethylation as a biomarker associated with poor prognosis. However, the effect of p53 has not been considered as a covariate in these attempts. Therefore, we further explored prognostic implication of L1 methylation with the addition of p53 expression status. In univariate survival analysis, intensity group 1 showed prolonged overall survival (OS) and disease-free survival (DFS) when compared with the respective one of intensity group 0 (P = 0.037 and P = 0.018, respectively; Figure 4A). When intensity group 1 was compared with all other groups combined, intensity group 1 exhibited marginally better OS than all other intensity groups (P = 0.052, Figure 4B). Intensity group 1 also had favorable prognosis for DFS compared with all other intensity groups (P = 0.030). Multivariate analysis reveals that L1 methylation level, lymphatic invasion, and pTNM stage were independent prognostic factors in OS and DFS. On the other hand, p53 intensity was not a prognostic factor when adjusted for pTNM stage, lymphatic invasion, venous invasion, perineural invasion, and L1 methylation level (Table 2). Also, we analyzed patient survival according to L1 methylation status in each p53 intensity subset (Figure 5). These results confirmed that L1 methylation level was a superior prognostic marker in AGC. However, we clearly identified the potential interaction between p53 expression and L1 methylation (Figure 2). From these findings, we decided to investigate the interaction of p53 expression and L1

methylation in vitro.

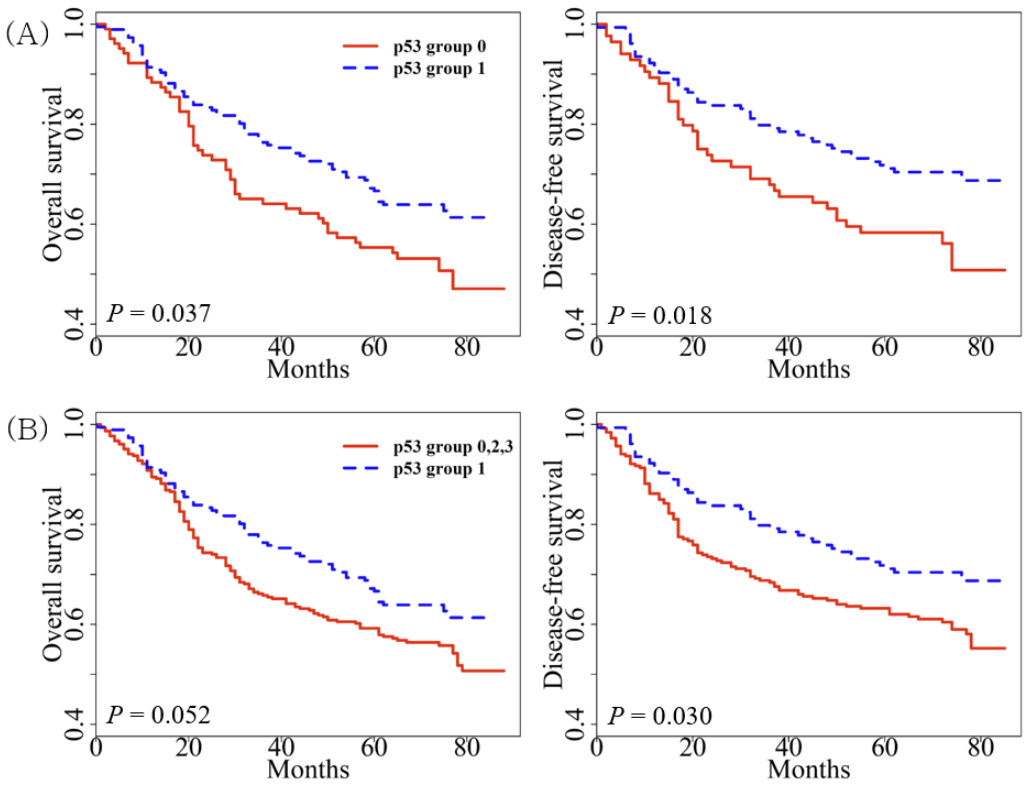

Fig. 4. Kaplan-Meier curve with a log rank test for p53 intensity.

(A) p53 intensity group 1 versus group 0 in overall survival (OS) and disease-free survival (DFS).

(B) All AGC samples were divided into two categories (p53 intensity group 1 versus group 0, 2, and 3) for survival analysis of overall survival (OS) and disease-free survival (DFS).

Table 2. Multivariate survival analysis.

Overall survival			
Variables	Hazard ratio	95% CI	*P* value
pTNM	1.955	1.429-2.673	<0.001
Lymphatic invasion	1.719	1.126-2.624	0.012
Venous invasion	13.49	0.936-1.946	0.109
Perineural invasion	1.228	0.862-1.750	0.255
p53 intensity	0.877	0.599-1.285	0.501
L1 methylation	0.566	0.381-0.841	0.005
Disease-free survival			
Variables	Hazard ratio	95% CI	*P* value
pTNM	1.963	1.435-2.684	<0.001
Lymphatic invasion	1.758	1.149-2.689	0.009
Venous invasion	1.329	0.9179-1.924	0.132
Perineural invasion	1.145	0.806-1.628	0.449
p53 intensity	0.859	0.587-1.255	0.432
L1 methylation	0.979	0.962-0.996	0.015

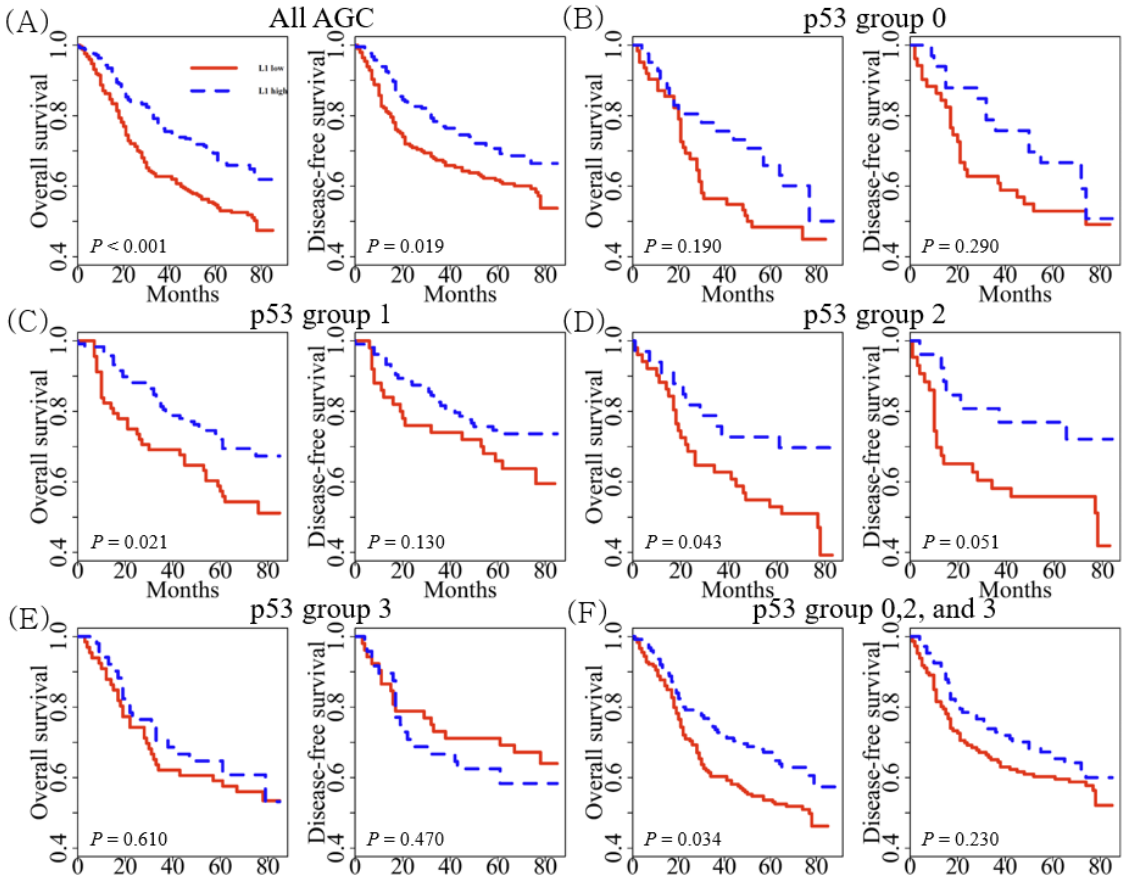

Fig. 5. Kaplan-Meier survival curves were compared between two groups using a log rank test to determine difference of patient survival according to L1 methylation status in each p53 intensity group.

(A) All AGC samples were included.

(B) AGC samples with negative p53 expression (intensity group 0)

(C) AGC samples with p53 intensity group 1

(D) AGC samples with p53 intensity group 2

(E) AGC samples with p53 intensity group 3

(F) All AGC samples except p53 intensity group 1 (group 0, 2, and 3)

Cell line selection and study design

To investigate the interaction between p53 expression and L1 methylation in vitro, we screened gastric cancer cell lines for their expression, mutation and copy number variation of *TP53* gene from cBioPortal (http://www.cbioportal.org) and selected *TP53*-null KATOIII and AGS carrying wild type *TP53* for functional analysis of p53 (Table3). As shown in Figure 6A and Table3, only KATOIII cell line showed complete loss of p53 expression since *TP53* gene was deleted. AGS and KATOIII were stably transfected with L1 plasmid DNA and KATOIII cells were transfected with *TP53* plasmid DNA sequentially by electroporation. Since AGS has endogenous wild type *TP53*, we first knocked down wild type *TP53* expression by shRNA from AGS which were already transfected with L1 plasmid and then re-introduced wild type *TP53* or mutant type *TP53*. Genomic DNA was extracted from the transfected cell line. DNA samples were then subjected to bisulfite conversion and subsequent pyrosequencing methylation assay for measuring L1 methylation level (Figure 6B).

Table3. The *TP53* status in gastric cancer cell line from cBioPortal online database.

	Gene expression	Mutation	Copy number status
SNU-601	2.174	No mutation	gain
SNU-1	-0.137	No mutation	no change
Hs746t	-2.522	K319*	gain
KATOIII	-2.903	Gross deletion	homozygous deletion
SNU-668	0.490	S215N	hemizygous deletion
AGS	-0.303	No mutation	no change
RERF-GC-1B	-2.678	R213*	hemizygous deletion
SNU-719	1.625	No mutation	no change

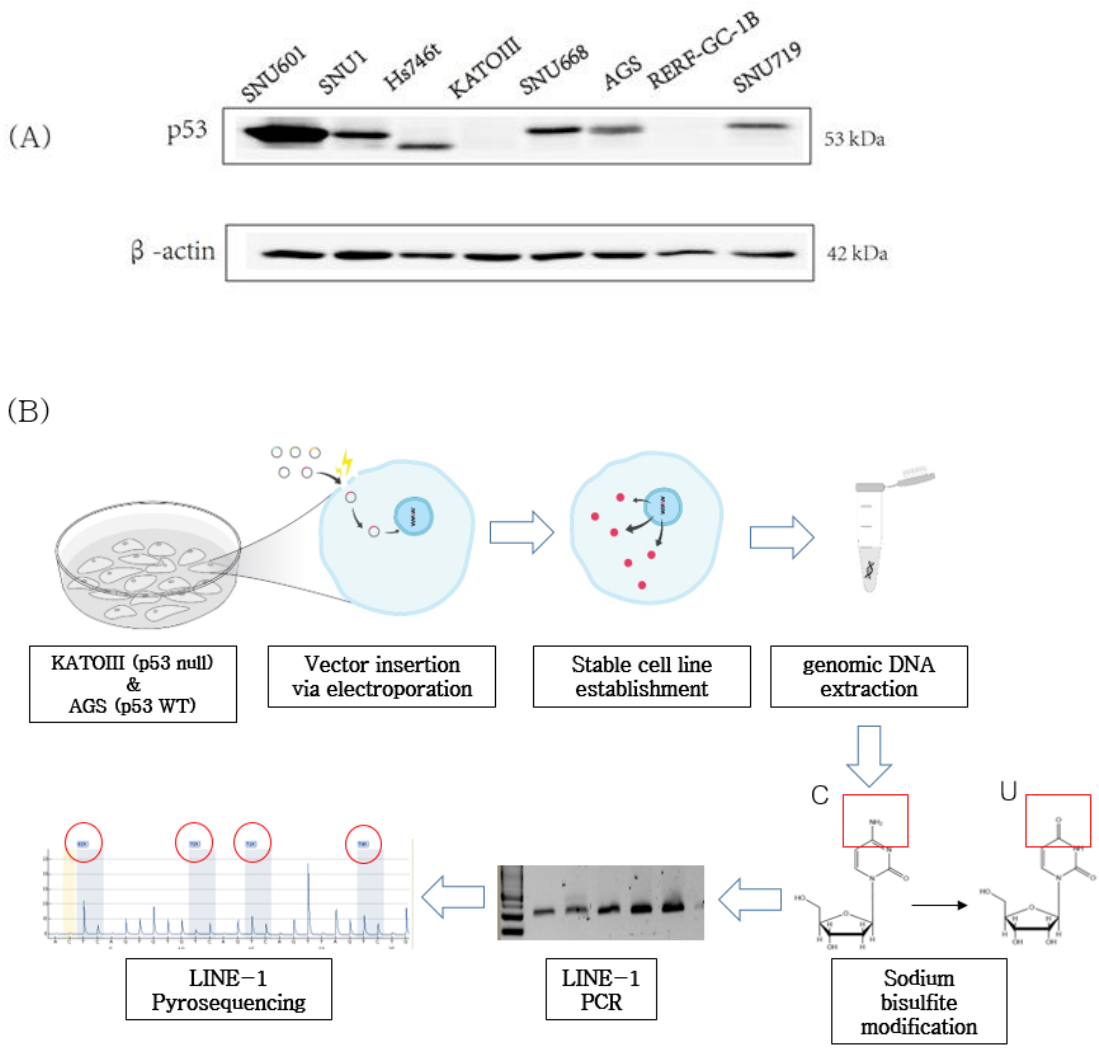

Fig. 6. Cell line selection and study design

(A) p53 protein expression in gastric cancer cell lines.

(B) KATOIII and AGS were stably transfected with L1 and *TP53* plasmid vectors. Genomic DNA samples from transfected cells were subjected to bisulfite conversion and subsequent pyrosequencing methylation assay.

Evaluation of transfection

To test our hypothesis, we established stable cell lines which express wild type or mutant type p53 protein with two different schemes in KATOIII and AGS cells. Briefly, wild type or mutant type *TP53* plasmids were introduced into KATOIII which were already transfected with wild type pLRE3-mEGFP1 plasmid for identifying stable L1 expression with green fluorescence. After complete G418 selection (antibiotic resistance marker in *TP53* plasmids), several colonies were chosen and examined for protein expression by western blot. p53 protein bands were detected from three types of mutant *TP53* (V143A, R175H, and R249S)-transfected cells. However, we failed to detect expression of wild type p53 despite our effort of evaluating over 20 colonies of wild type *TP53*-transfected cells (Figure 7A, left). In case of AGS, we knocked down wild type p53 expression by shRNA from AGS which were initially transfected with wild type pLRE3-mEGFP1 plasmid and re-introduced wild type *TP53* or mutant type *TP53*. Knock down of *TP53* expression and stable transfection of wild type *TP53* and mutant type *TP53* plasmids were confirmed in western blot analysis (Figure 7A, right). Next, we performed RT-PCR to detect *TP53* RNA transcripts in KATOIII. Wild type *TP53* transcript (Lane 13) was not detected while transcriptions of mutant type *TP53* were confirmed (Figure 7B). Lastly, we conducted PCR with universal primer sets in *TP53* plasmids and *TP53* primer sets for investigating the presence of pCMV-NEO-BAM

plasmid which wild type and mutant types of *TP53* was cloned into and for identifying the presence of *TP53* DNA in KATOIII, respectively. In the top panel, from lane 6 to 9, approximately 500bp of PCR products (representing pCMV-NEO-BAM vector) were detected from all *TP53* transfected cells. (Figure 7C, top panel). However, approximately 476bp of PCR product (representing *TP53* DNA) was not detected from wild type *TP53* transfected cells. (Figure 7C, bottom, lane 6). Although wild type *TP53* from KATOIII expressing wild type L1 could not be detected by western blotting and RT-PCR, we investigated DNA trace of *TP53* by polymerase chain reaction (PCR) and detected p53 plasmids integrated in genomic region of the cell.

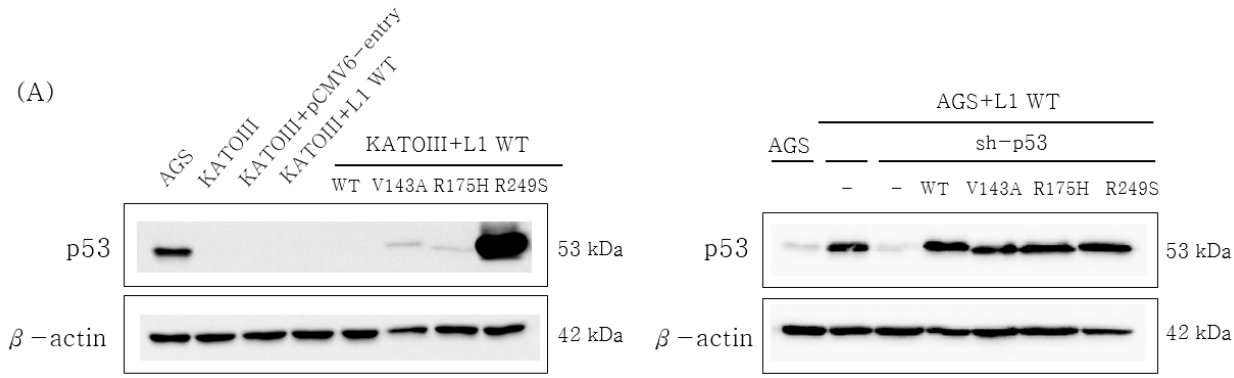
(A)
AGS
KATOIII
KATOIII+pCMV6-entry
KATOIII+L1 WT
KATOIII+L1 WT
WT V143A R175H R249S
p53
β-actin
53 kDa
42 kDa
AGS+L1 WT
AGS
sh-p53
- - WT V143A R175H R249S

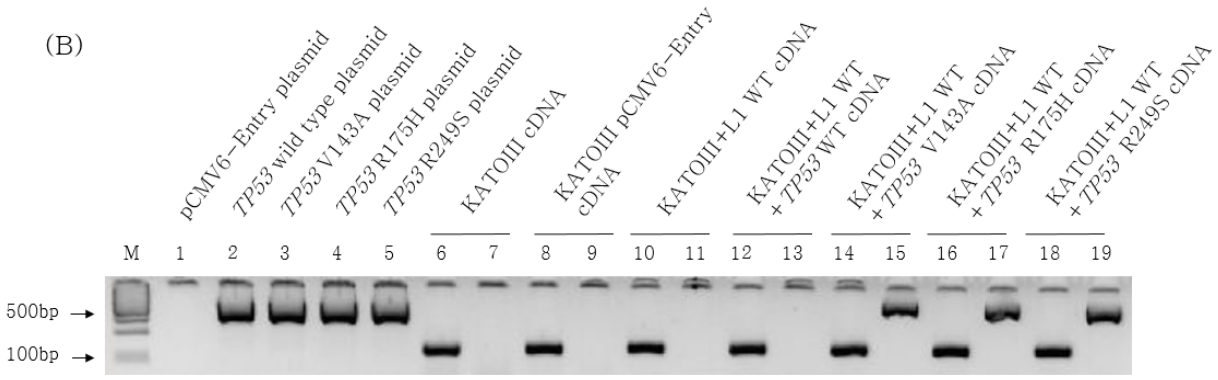
(B)
pCMV6-Entry plasmid
TP53 wild type plasmid
TP53 V143A plasmid
TP53 R175H plasmid
TP53 R249S plasmid
KATOIII cDNA
KATOIII pCMV6-Entry cDNA
KATOIII+L1 WT cDNA
KATOIII+L1 WT + TP53 WT cDNA
KATOIII+L1 WT + TP53 V143A cDNA
KATOIII+L1 WT + TP53 R175H cDNA
KATOIII+L1 WT + TP53 R249S cDNA
M 1 2 3 4 5 6 7 8 9 10 11 12 13 14 15 16 17 18 19
500bp
100bp

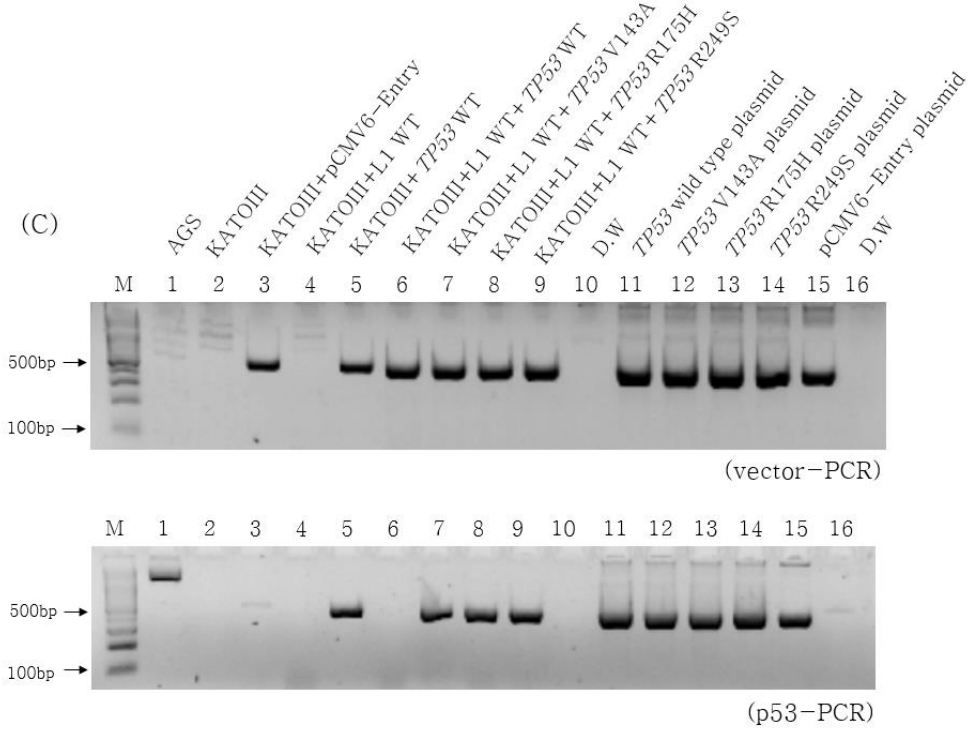
(C)
AGS
KATOIII
KATOIII+pCMV6-Entry
KATOIII+L1 WT
KATOIII+ TP53 WT
KATOIII+L1 WT+ TP53 WT
KATOIII+L1 WT+ TP53 V143A
KATOIII+L1 WT+ TP53 R175H
KATOIII+L1 WT+ TP53 R249S
D.W
TP53 wild type plasmid
TP53 V143A plasmid
TP53 R175H plasmid
TP53 R249S plasmid
pCMV6-Entry plasmid
D.W
M 1 2 3 4 5 6 7 8 9 10 11 12 13 14 15 16
500bp
100bp
(vector-PCR)
M 1 2 3 4 5 6 7 8 9 10 11 12 13 14 15 16
500bp
100bp
(p53-PCR)

Fig. 7. Evaluation of transfection by western blot, RT-PCR (reverse transcription-polymerase chain reaction) and PCR (polymerase chain reaction) analysis

(A) p53 protein expression level in KATOIII (left) and AGS (right) transfected with wild type or mutant types of *TP53* by western blot.

(B) Expression of p53 in KATOIII transfected with wild type or mutant types of *TP53* by RT-PCR.

[Lane 1~5: pCMV6-Entry vector, pCMV-NEO-BAM-p53 wild type vector and pCMV-NEO-BAM-p53 mutant type vectors (V143A, R175H, and R249S respectively), Lane 6 to 11: cDNA from KAOTIII (Lane 6 and 7), KATOIII+ pCMV6-Entry (Lane 8 and 9), and KATOIII+ L1 WT (Lane 10 and 11). Lane 12 to 19: cDNA from KATOIII expressing wild type L1 transfected with wild type p53 (Lane 12 and 13), V143A (Lane 14 and 15), R175H (Lane 16 and 17) and R249S (Lane 18 and 19) (Lane 6, 8, 10, 12, 14, 16, and 18: PCR with GAPDH primer)].

(C) Genomic DNA was extracted and amplified by two different primer sets in PCR to determine whether plasmid vector and *TP53* gene have been integrated in genomic region of the cell.

(Lane 1: AGS, Lane 2: KATOIII, Lane 3: KATOIII+ pCMV6-Entry, Lane 4: KATOIII+ L1 Wild type, Lane 5: KATOIII+ p53 wild type, Lane 6: KATOIII+ L1 WT+ p53 Wild type, Lane 7~9: KATOIII+ L1 WT+ p53 mutant type (V143A, R175H, and R249S, respectively). Lane 11~15: pCMV6-Entry vector, pCMV-NEO-BAM-p53 wild type vector, and pCMV-NEO-BAM-p53 mutant type vectors (V143A,

R175H, and R249S respectively). A 100bp DNA molecular weight size marker (Bioneer) is indicated in the flanking lanes (M)).

L1 retrotransposition activity according to p53 mutation

To observe L1 expression levels by fluorescence, we transfected KATOIII and AGS with the pLRE3-mEGFP1 plasmid encoding a retrotransposition-competent L1 and its mutant pJM111-LRE3-mEGFP1 encoding a retrotransposition-incompetent L1 and selected stably integrated cells using puromycin. Next, we transfected the wild type and mutant type *TP53* (V143A, R175H and R249S) plasmids into KATOIII and *TP53*-knocked down AGS, both cell lines expressing recombinant L1, to investigate L1 expression depending on mutational status of *TP53*.

Construct of pLRE3-mEGFP1 plasmid and overview of L1 retrotransposition is illustrated in Figure 8A. The EGFP reporter gene is disrupted by an intron which has the same transcription orientation with L1. Thus, EGFP can be expressed from CMV promoter only when L1 plasmid is transcribed from its native promoter in 5' UTR, spliced to remove the intron and target-primed retrotranspostion occurs. In other words, EGFP-positive cells can be detected only if the pLRE3 transcript undergoes a successful retrotransposition(18). In this sense, EGFP positive cells represent relative L1 expression level.

We confirmed EGFP protein level by western blot (Figure 8B). Since it is difficult to detect L1 protein expression because of its unconventional translation mechanism(19, 20), EGFP expression was considered as a surrogate for exogenous L1 expression. After

detecting high level of EGFP protein in *TP53* mutant R175H-expressing KATOIII and AGS by western blot (Figure 8B), we then examined L1 retrotransposition activity in KATOIII cells by fluorescent microscopy and FACS (Figure 8C top and Figure 8D left). For analyzing L1 retrotransposition activity from AGS, we observed EGFP positive cells by fluorescent microscopy and quantified the EGFP protein band intensity relative to actin band (Figure 8C bottom and Figure 8D right). Consistent with the results from western blot, we detected more EGFP positive cells in R175H mutant *TP53* cells than in V143A and R249S mutant *TP53* cell both in KATOIII and AGS.

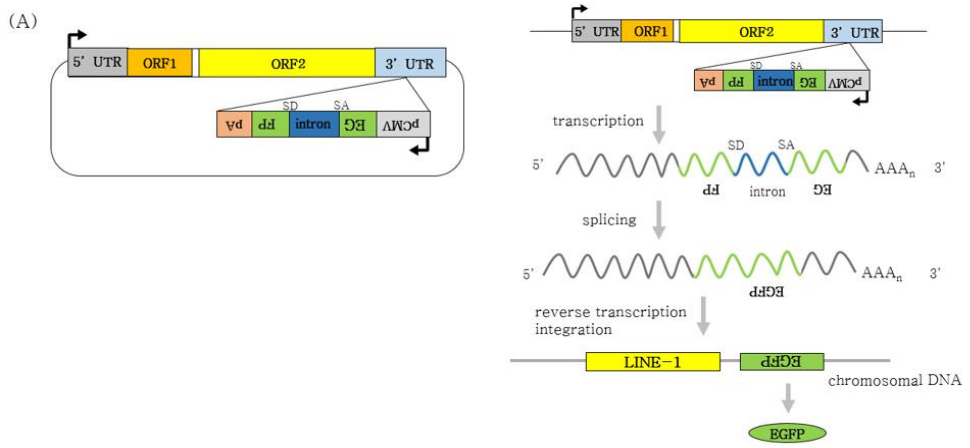
(A)
5' UTR
ORF1
ORF2
3' UTR
pA
RP
intron
EG
pCMV
SD
SA
transcription
splicing
reverse transcription
integration
LINE-1
chromosomal DNA
EGFP

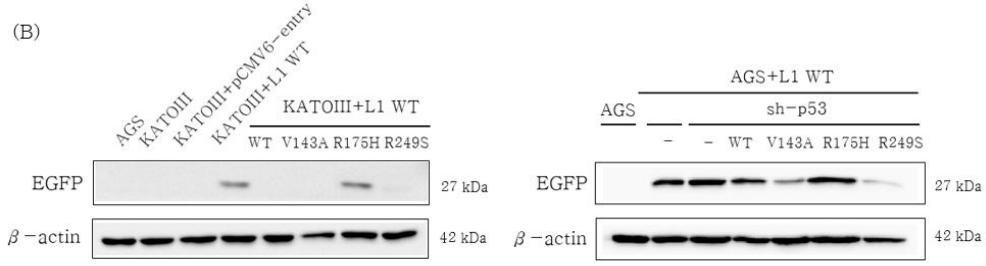
(B)
AGS
KATOIII
KATOIII+pCMV6-entry
KATOIII+L1 WT
KATOIII+L1 WT
WT V143A R175H R249S
AGS+L1 WT
AGS
sh-p53
EGFP
β-actin
27 kDa
42 kDa

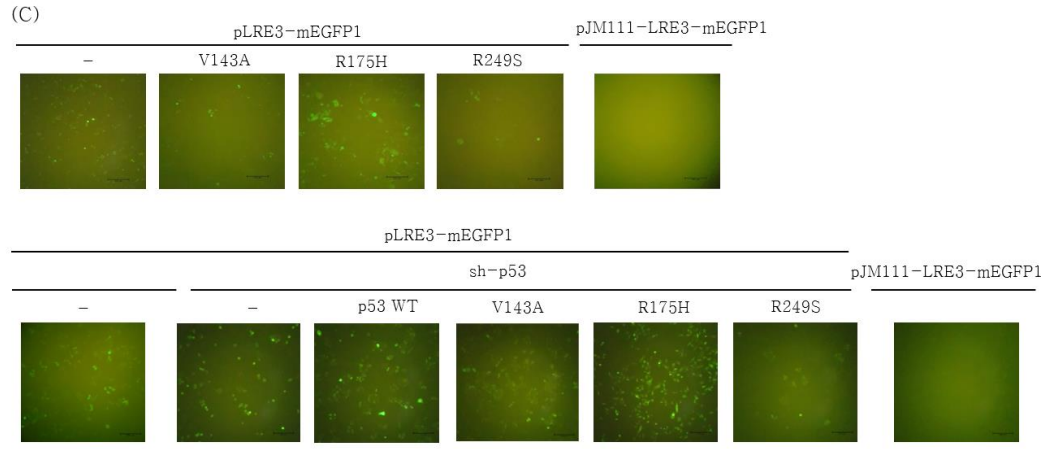
(C)
pLRE3-mEGFP1
pJM111-LRE3-mEGFP1
V143A
R175H
R249S
sh-p53
p53 WT

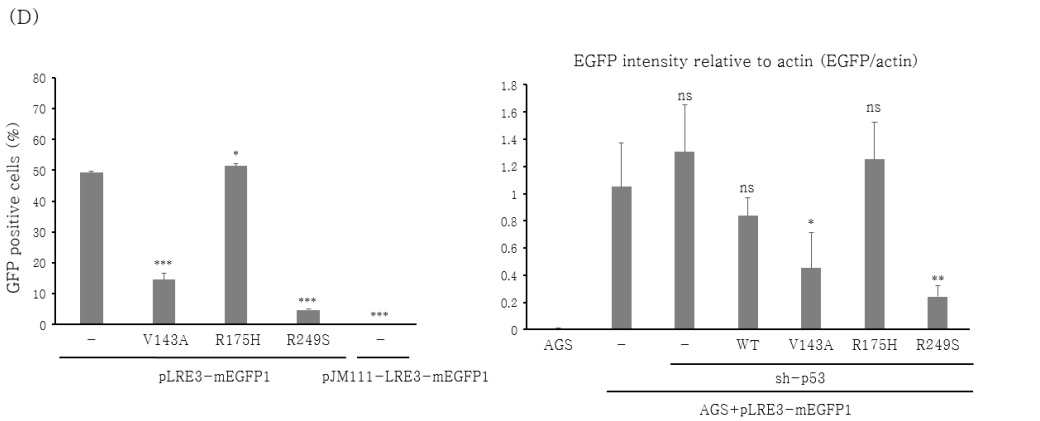
(D)
GFP positive cells (%)
EGFP intensity relative to actin (EGFP/actin)
V143A
R175H
R249S
pLRE3-mEGFP1
pJM111-LRE3-mEGFP1
AGS
WT
sh-p53
AGS+pLRE3-mEGFP1
ns

Fig. 8. L1 expression level in p53-transfected KATOIII and AGS gastric cancer cell line

(A) Schematic diagram of the pLRE3-mEGFP1 construct (left) and rationale of the L1-retrotransposition assay (right). The EGFP retrotransposition reporter cassette is cloned into the 3'UTR of L1 in the antisense orientation. The cassette consists of the CMV promoter (pCMV), the TK poly(A) signal (pA) and the EGFP gene interrupted by a sense orientation intron(intron) with the splice donor (SD) and splice acceptor (SA).

(B) EGFP protein expression levels from p53-transfected KATOIII (left) and AGS(right).

(C) Green Fluorescence Protein observed by fluorescence microscope from p53-transfected KATOIII (top) and AGS (bottom) (scale bar: 100μm).

(D) Quantification of EGFP positive (+) cells by GFP fluorescence-activated cell sorter (FACS) analysis from p53-transfected KATOIII (left) and quantification of EGFP intensity by western blot from p53-transfected AGS (right).

(*: $P < 0.05$, **: $P < 0.01$, ***: $P < 0.001$)

L1 methylation level according to p53 mutation

To explore whether L1 methylation status is influenced by *TP53* mutation status, we examined the methylation level of L1 in *TP53* -transfected KATOIII and AGS cells by pyrosequencing. L1 methylation tended to be different depending on the type of *TP53* mutation and was highest in KATOIII cells transfected with *TP53* mutant R175H (Figure 9A). In AGS cells, L1 methylation level was slightly reduced when *TP53* was knocked down. Reintroduction of wild type *TP53* caused a significant decrease in L1 methylation level. L1 methylation levels in *TP53*-knocked down AGS cells were variable depending on mutant type *TP53* (V143A, R175H, and R249S) (Figure 9B).

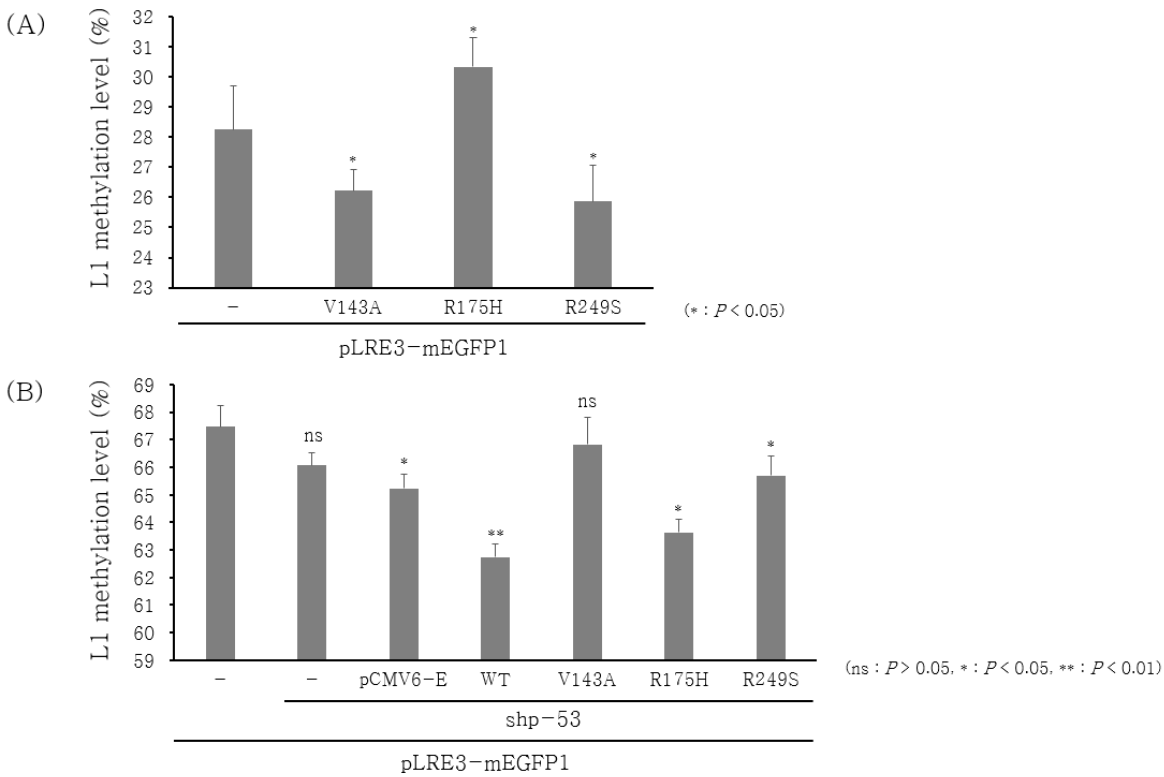

Fig. 9. L1 methylation level in p53-transfected KATOIII and AGS gastric cancer cell line

(A) Mean methylation levels of the four serial CpG sites of L1 for KATOIII cells expressing mutant type p53 (V143A, R175H, and R249S).

(B) Mean methylation levels of the four L1 CpG sites for AGS cell line expressing wild type and mutant type p53 (V143A, R175H, and R249S).

Discussion

In our previous studies, L1 methylation level was found to be a reliable independent prognostic biomarker in which a low methylation status was associated with worse clinical outcome of AGC patients(17, 18). In our current investigation, intensity or expression status of p53 has also shown prognostic value in univariate analysis. Although genomic analysis of *TP53* mutation was not performed in this study, previous studies have reported that scattered type-p53 immunohistochemical staining, equivalent to that of intensity group 1 in our study, was genetically wild type in gastric cancer(21), and another study stated that mutated *TP53* samples were immunopositive (group 2 and 3) or negative (group 0)(22). Therefore, we deduced that immunohistochemical status of p53 is a representative of its mutation status. However, in multivariate analysis, p53 intensity no longer maintained its prognostic implications. These findings indicate that despite the potential interaction between p53 and L1 methylation, L1 methylation comes out on top as a superior prognostic marker in AGC.

To investigate the correlation between *TP53* mutation status and L1 methylation in vitro, we used KATOIII cell line carrying the gross deletion of *TP53* and AGS cell line carrying wild type *TP53.* Briefly, wild type *TP53* and mutant type *TP53* (V143A, R175H, and R249S) plasmids were introduced to KATOIII which was already transfected

with pLRE3-mEGFP1(wild type L1 plasmid) or its mutant, pJM111-LRE3-mEGFP1. For AGS, wild type *TP53* and mutant type *TP53* plasmids were introduced to AGS which was already transfected with wild or mutant type L1 and *TP53* shRNA. It has been reported that the vast majority of mutant *TP53* has point mutations in DNA-binding domain and R175H and R249S are referred to as hot spot mutations that disrupt tumor suppressive activity(23). These *TP53* mutations are now known to have oncogenic properties instead of tumor suppressive roles.

In this study, we used the EGFP reporter cassette to observe L1 expression by green fluorescence. Since EGFP reporter gene is disrupted by an intron which has same transcription orientation with L1, EGFP can be expressed only when L1 plasmid undergoes a successful retrotransposition(18). Thus, we could confirm that L1 plasmid was successfully integrated in the genomic region of cell by fluorescence microscope. After we confirmed integration of wild type L1 plasmid into KATOIII and AGS, wild type and mutant type *TP53* were additionally transfected into KATOIII expressing L1 and AGS expressing L1 and p53 shRNA. Although all *TP53* plasmid DNA were detected by PCR, wild type *TP53* was not detected by RT-PCR and western blot in KATOIII. According to findings from GFP fluorescence, V143A and R249S mutant *TP53*-transfected KATOIII cells showed decreased L1 expression and R175H mutant p53-transfected KATOIII showed elevated L1 expression compared to KATOIII expressing L1. *TP53*-knocked down AGS cells showed

results of GFP fluorescence comparable with those of KATOIII. Finally, we measured L1 mean methylation level of four serial CpG sites by pyrosequencing. Consistent with FACS analysis, only R175H mutant-transfected cells had different expression level of EGFP from other *TP53* mutants in KATOIII. Unlike R175H mutant, V143A and R249S mutants reduced L1 methylation in KATOIII. In AGS, wild type p53 mutant type p53s all differently regulated L1 methylation. Importantly, L1 methylation tended to be different depending on the type of *TP53* mutation both in KATOIII and AGS. However, the data presented are not sufficient to cover the overall effect of p53 over L1.

As a limitation of this study, wild type p53 was not detected at protein level from KATOIII transfected with both L1 and wild type *TP53*. Apparently, cell morphology and growth has significantly changed when wild type *TP53* was introduced into *TP53*-null KATOIII. Introduction of wild type *TP53* can cause a severe damage to the *TP53*-deleted KATOIII, probably giving a similar effect expected in *TP53*-inducing gene therapy(24). To this end, we designed a new experimental scheme with AGS, a cell line that expresses wild type *TP53*. Briefly, we knocked down wild type *TP53* expression by shRNA and re-introduced wild type p53 or mutant type p53.

Altogether, we found that L1 methylation level was strongly correlated with p53 expression status in total AGC cohort and that in in-vitro study, L1 methylation level or L1 expression level were

differentially altered depending on the type of *TP53* mutants. However, the underlying mechanisms should be further validated in order to elaborate the interaction between p53 and L1.

References

1. Yoo CH, Noh SH, Shin DW, Choi SH, Min JS. Recurrence following curative resection for gastric carcinoma. Br J Surg. 2000;87(2):236-42.
2. Chalitchagorn K, Shuangshoti S, Hourpai N, Kongruttanachok N, Tangkijvanich P, Thong-ngam D, et al. Distinctive pattern of LINE-1 methylation level in normal tissues and the association with carcinogenesis. Oncogene. 2004;23(54):8841-6.
3. Harris CR, Dewan A, Zupnick A, Normart R, Gabriel A, Prives C, et al. p53 responsive elements in human retrotransposons. Oncogene. 2009;28(44):3857-65.
4. Karpf AR, Matsui S. Genetic disruption of cytosine DNA methyltransferase enzymes induces chromosomal instability in human cancer cells. Cancer Res. 2005;65(19):8635-9.
5. Song YS, Kim Y, Cho NY, Yang HK, Kim WH, Kang GH. Methylation status of long interspersed element-1 in advanced gastric cancer and its prognostic implication. Gastric Cancer. 2016;19(1):98-106.
6. Olivier M, Hollstein M, Hainaut P. TP53 mutations in human cancers: origins, consequences, and clinical use. Cold Spring Harbor perspectives in biology. 2010;2(1):a001008.
7. Toledo F, Wahl GM. Regulating the p53 pathway: in vitro hypotheses, in vivo veritas. Nature reviews Cancer. 2006;6(12):909-23.
8. Lawrence MS, Stojanov P, Mermel CH, Robinson JT, Garraway LA, Golub TR, et al. Discovery and saturation analysis of cancer genes across 21 tumour types. Nature. 2014;505(7484):495-501.
9. Zhu J, Sammons MA, Donahue G, Dou Z, Vedadi M, Getlik M, et al. Gain-of-function p53 mutants co-opt chromatin pathways to drive cancer growth. Nature. 2015;525(7568):206-11.
10. Muller PA, Vousden KH, Norman JC. p53 and its mutants in tumor cell migration and invasion. The Journal of cell biology. 2011;192(2):209-18.
11. Do PM, Varanasi L, Fan S, Li C, Kubacka I, Newman V, et al. Mutant p53 cooperates with ETS2 to promote etoposide resistance. Genes Dev. 2012;26(8):830-45.
12. Freed-Pastor WA, Mizuno H, Zhao X, Langerod A, Moon SH, Rodriguez-Barrueco R, et al. Mutant p53 disrupts mammary tissue architecture via the mevalonate pathway. Cell. 2012;148(1-2):244-58.
13. Zhang C, Liu J, Liang Y, Wu R, Zhao Y, Hong X, et al. Tumour-associated mutant p53 drives the Warburg effect. Nature communications. 2013;4:2935.
14. Wylie A, Jones AE, D'Brot A, Lu WJ, Kurtz P, Moran JV, et al. p53 genes function to restrain mobile elements. Genes Dev. 2016;30(1):64-77.
15. Weisenberger DJ, Campan M, Long TI, Kim M, Woods C, Fiala E, et al. Analysis of repetitive element DNA methylation by MethyLight. Nucleic Acids Res. 2005;33(21):6823-36.

16. Tellez CS, Shen L, Estecio MR, Jelinek J, Gershenwald JE, Issa JP. CpG island methylation profiling in human melanoma cell lines. Melanoma research. 2009;19(3):146-55.
17. Kim Y, Wen X, Jeong S, Cho NY, Kim WH, Kang GH. Combinatory low methylation statuses of SAT-alpha and L1 are associated with shortened survival time in patients with advanced gastric cancer. Gastric Cancer. 2018.
18. Garcia-Perez JL, Morell M, Scheys JO, Kulpa DA, Morell S, Carter CC, et al. Epigenetic silencing of engineered L1 retrotransposition events in human embryonic carcinoma cells. Nature. 2010;466(7307):769-73.
19. Alisch RS, Garcia-Perez JL, Muotri AR, Gage FH, Moran JV. Unconventional translation of mammalian LINE-1 retrotransposons. Genes Dev. 2006;20(2):210-24.
20. Doucet AJ, Hulme AE, Sahinovic E, Kulpa DA, Moldovan JB, Kopera HC, et al. Characterization of LINE-1 ribonucleoprotein particles. PLoS Genet. 2010;6(10).
21. Ando K, Oki E, Saeki H, Yan Z, Tsuda Y, Hidaka G, et al. Discrimination of p53 immunohistochemistry-positive tumors by its staining pattern in gastric cancer. Cancer medicine. 2015;4(1):75-83.
22. Murnyak B, Hortobagyi T. Immunohistochemical correlates of TP53 somatic mutations in cancer. Oncotarget. 2016;7(40):64910-20.
23. Soussi T, Wiman KG. TP53: an oncogene in disguise. Cell death and differentiation. 2015;22(8):1239-49.
24. Valente JFA, Queiroz JA, Sousa F. p53 as the Focus of Gene Therapy: Past, Present and Future. Curr Drug Targets. 2018;19(15):1801-17.

국 문 초 록

p53은 종양억제단백질로서, DNA 복구, 세포 주기 억류, 노화, 혈관신생 그리고 세포자살 유도와 같은 종양형성을 막는 중요한 생물학적 과정을 조절한다. p53은 많은 암에서 흔히 돌연변이가 일어나 있다. p53의 돌연변이는 단순히 야생형 p53의 기능을 잃는 것과 더불어, 새로운 돌연변이 기능을 얻게 되어 종양의 유지와 진행에 선택적인 이점을 준다. Long interspersed nuclear element-1 (LINE-1, L1)은 반복되는 DNA 서열로 인간 유전체의 약 17퍼센트를 구성한다. L1의 발현은 체세포에서 주로 5' 비번역 부위에 있는 CpG 지점이 메틸화됨에 따라 억제되지만 종양형성이 일어나면서 DNA 탈메틸화 과정에 의해 L1이 활성화된다. L1은 레트로트랜스포지션 활성이 있어서, 암의 중요한 특징인 유전체 불안정화에 기여할 수 있다. 반면에, p53은 유전체 안정화를 유지하는데 필수적이다. 다른 연구에서는 p53이 레트로트랜스포존의 활성을 억제함으로써 유전체 안정화를 유지하는 역할에 대해 밝혀왔다. 그러나, L1과 관련된 p53의 조절기능은 인간 위암에서 잘 밝혀지지 않았다. 또한 p53이 돌연변이 상태에 따라 L1의 발현을 다르게 조절하는지에 대해서도 불명확하다. p53 면역화학염색과 L1 파이로시퀀싱 실험으로부터, 우리는 L1 메틸화와 p53발현의 강력한 상관관계를 확인했다. 이를 통해, 우리는 p53 단백질이 L1 CpG섬 메틸화나 L1 발현과 관련이 있을 것이며, *TP53*의 돌연변이는 L1의 발현이나 DNA메틸화상태에 영향을 줄 것이라는 가설을 세웠다. 이 연구에서 우리는 *TP53*이 결손된 인간 위암세포주인 KATOIII와 야생형

*TP53*을 가진 AGS에서 p53이 L1의 발현이나 메틸화 정도를 조절하는 기작에 대해 검증했다. *TP53* 돌연변이의 종류에 따라 L1의 레트로트렌스포지션 활성이나 메틸화수준의 차이가 유발되었다. 우리의 결과를 입증하기 위해서는 후속 연구가 필요할 것이다.

주요어: p53, LINE-1, 메틸화, 파이로시퀀싱, 후성유전학, 위암, KATOIII

학 번: 2017-29457